

# NMR analysis of the magnetic structure of UNiGa<sub>5</sub>

Tetsuo Ohama\* and Masanori Hirano

*Graduate School of Science and Technology, Chiba University, Chiba 263-8522, Japan*

Satoru Noguchi

*Graduate School of Engineering, Osaka Prefecture University, Sakai 599-8531, Japan*

(Received 24 September 2004; published 11 March 2005)

We present NMR analysis of the magnetic structure of the itinerant antiferromagnet UNiGa<sub>5</sub>. We measured <sup>69,71</sup>Ga NMR spectra in the paramagnetic and antiferromagnetic phases and determined the quadrupole parameters and the internal fields at the Ga sites. Using a symmetry analysis of the internal fields based on magnetic groups and a representation analysis of magnetic structure, we have determined a collinear structure with the ordered moment along the *c* axis.

DOI: 10.1103/PhysRevB.71.094408

PACS number(s): 75.25.+z, 76.60.-k

## I. INTRODUCTION

Nuclear magnetic resonance (NMR) is a powerful probe in studies of magnetic,<sup>1</sup> charge,<sup>2</sup> and orbital ordering, and it is complementary to neutron and x-ray diffraction. For magnetic ordering, NMR for magnetic nuclear sites provides rich information about the magnitude and the direction of the ordered moment and the symmetry of magnetic orbitals such as *3d* and *4f*; such information is obtained from the magnitude and the direction of internal fields at the nuclear sites. And as for nonmagnetic nuclear sites, the breaking of time reversal and crystal symmetry at the magnetic transition can create internal fields at those sites or can split those sites into several groups of nonequivalent sites or both in the ordered phase. Thus, NMR for such nonmagnetic sites is sensitive to the symmetry of the sites or the arrangement of the ordered moment on neighboring magnetic ions. Particularly in commensurate antiferromagnets, in contrast to incommensurate ordering that leads to spatially modulated internal fields, the symmetry-breaking can induce only a few additional nonequivalent sites, so that those sites can be, in principle, resolved in NMR spectra. In that case NMR provides important information for determining the magnetic structure.

To examine internal fields at nuclear sites, one usually measures a zero-field NMR spectrum or examines angular dependence of an NMR spectrum in external fields. In those analyses of magnetic structure carried out to date, assuming structure models and hyperfine coupling tensors in appropriate forms, one used an internal field calculation and a symmetry analysis together to find the structure that agrees with the NMR measurements. That heuristic approach is, however, inefficient for searching for the magnetic structure before it is known. In this paper, we present a systematic NMR analysis of magnetic structure: we find possible magnetic structures with a general analysis based on space group representations<sup>3-5</sup> and sort out the structures compatible with the NMR spectrum with a symmetry analysis of the internal field based on magnetic groups. This analysis is independent of the intensity analysis of neutron magnetic reflections, and thus it should be useful as a complementary tool for magnetic structure studies. We applied it to our <sup>69,71</sup>Ga NMR measurements in the itinerant antiferromagnet UNiGa<sub>5</sub> and have determined the magnetic structure of this compound.

As shown in Fig. 1, UNiGa<sub>5</sub> has the tetragonal HoCoGa<sub>5</sub> structure (space group *P4/mmm*),<sup>6</sup> containing two inequivalent Ga sites: Ga(1) with point symmetry of *4/mmm* and Ga(2) with *mm2*. Room temperature lattice parameters and atomic coordinates<sup>7</sup> are given in Table I. The magnetic susceptibility and the specific heat measurements suggest magnetic ordering at the Néel temperature  $T_N=86\text{K}$ .<sup>8,9</sup> Neutron diffraction measurements revealed a type-II antiferromagnetic ordering with the propagation vector  $\mathbf{k}=\left[\frac{1}{2}\frac{1}{2}\frac{1}{2}\right]$ .<sup>10</sup> They also found that the observed intensities of magnetic reflections are reproduced by the magnetic structure with the magnetic moment on the U ions along the *c* axis better than by the structure with the moment along the *a* axis. Our NMR analysis, which is independent of this reflection intensity analysis, gives the same structure as described below.

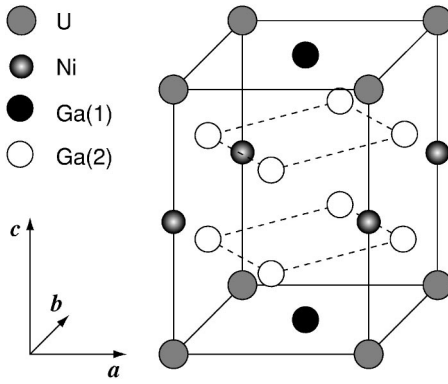
## II. EXPERIMENTAL PROCEDURES

The powder sample used in the present study was prepared by arc-melting of the constituent elements in an argon atmosphere, followed by annealing at 870 °C for one week. The ingot was then finely powdered for the NMR measurements. A home-built pulsed spectrometer was used for the measurements; the NMR spectra in the paramagnetic phase were taken by integrating a spin-echo signal with sweeping the external magnetic field, and in the antiferromagnetic phase the frequency spectra were taken in zero external field.

## III. EXPERIMENTAL RESULTS

### A. NMR spectrum in the paramagnetic phase

Figure 2 shows the <sup>69,71</sup>Ga ( $I=3/2$ ) NMR spectrum at 110 K in the paramagnetic phase. The observed spectrum consists of typical powder patterns of quadrupolar splitting by symmetric field gradient for the Ga(1) sites and by asymmetric one for the Ga(2) sites in agreement with the site symmetry of these Ga sites. We determined the principal values of the NMR shift tensor  $K_X$ ,  $K_Y$ ,  $K_Z$ , and the quadrupole parameters, the quadrupole frequency  ${}^{71}\nu_Q$  and the asymmetry parameter  $\eta$  for <sup>71</sup>Ga nuclei, by the second-order perturbation analysis<sup>11</sup> as given in Table II. The *X*, *Y*, and *Z* axes are taken as the principal axes of the field gradient

FIG. 1. Crystal structure of UNiGa<sub>5</sub>.

tensor  $V_{\alpha\beta}$  so that  $|V_{ZZ}| \geq |V_{YY}| \geq |V_{XX}|$ .<sup>1</sup> The quadrupole frequency  ${}^{69}\nu_Q$  for  ${}^{69}\text{Ga}$  nuclei is deduced from the ratio of the quadrupole moments of  ${}^{69}\text{Ga}$  and  ${}^{71}\text{Ga}$  nuclei  ${}^{69}Q/{}^{71}Q = 1.5869$ ,<sup>12</sup> also shown in Table II. The deduced quadrupole parameters agree with a single-crystal NMR measurement.<sup>13</sup>

We examine the orientation of the X, Y, and Z axes relative to the crystalline axes by considering the site symmetry. The Ga(1) sites with symmetric field gradient have a fourfold axis along the crystalline  $c$  axis, and thus the  $c$  axis should correspond to the maximal principal-axis Z. We can take the X and Y axes parallel to the  $a$  and  $b$  axes, respectively. For the Ga(2) sites with asymmetric field gradient, each of the principal axes should be perpendicular to one of the two mirror planes or parallel to the twofold axis, hence it is parallel to one of the crystalline axes. We cannot, however, determine to which crystalline axis each of the principal axes corresponds only from the site symmetry. We will discuss it later.

### B. Zero-field NMR spectrum in the antiferromagnetic phase

In the paramagnetic phase, four resonance lines are expected in zero-field spectra: for each of  ${}^{69}\text{Ga}$  and  ${}^{71}\text{Ga}$  nuclei (both  $I=3/2$ ), one line for the Ga(1) sites and another for the Ga(2) sites. In the antiferromagnetic phase, the breaking of time reversal and crystal symmetry at the phase transition can lead to additional lines in the spectrum; those lines are ascribed to a change in the site symmetry or the appearance of an internal field at the Ga sites or the appearance of non-equivalent Ga sites.

Figure 3 shows the  ${}^{69,71}\text{Ga}$  NMR spectrum in zero external field at 1.5 K in the antiferromagnetic phase. Twelve

TABLE I. Lattice parameters and atomic coordinates of UNiGa<sub>5</sub> at 300 K (Ref. 7).

| $P4/mmm: a=4.2380 \text{ \AA}, c=6.7864 \text{ \AA}$ |      |     |     |        |
|--|------|-----|-----|--------|
|  | Site | $x$ | $y$ | $z$    |
| U  | 1a   | 0   | 0   | 0      |
| Ni   | 1b   | 0   | 0   | 1/2    |
| Ga(1)  | 1c   | 1/2 | 1/2 | 0      |
| Ga(2)  | 4i   | 0   | 1/2 | 0.3074 |

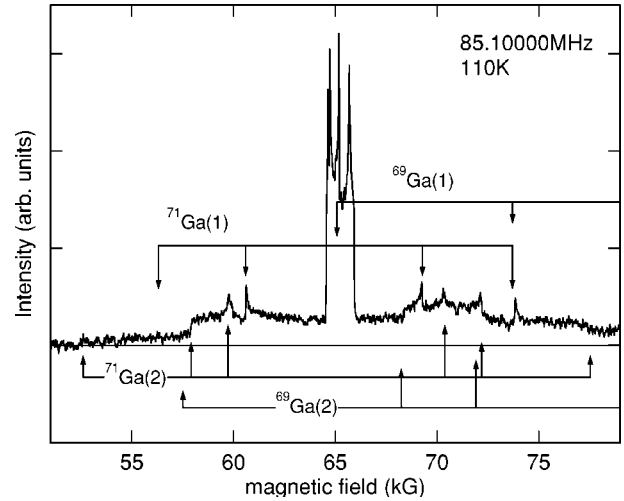


FIG. 2.  ${}^{69,71}\text{Ga}$  NMR spectrum at 110 K in the paramagnetic phase. Satellite singularities are shown with arrows.

sharp resonance lines are observed in the frequency range between 7 and 50 MHz; a typical full width at half-maxima  $\Delta$  is about 0.1 MHz. The resonance frequencies  $\nu_{\text{obs}}$  and  $\Delta$  are listed in Table III.

To deduce the quadrupole parameters and the internal field  $\mathbf{B}^{\text{int}}$  from this spectrum, we assign these resonance lines to the crystalline Ga sites. Consider first the lines 1 and 2. The frequencies of these lines are close to  ${}^{71}\nu_Q$  and  ${}^{69}\nu_Q$  at the Ga(1) sites in the paramagnetic phase, respectively, and the ratio of the frequencies 1.5862 is also very close to  ${}^{69}Q/{}^{71}Q = 1.5869$ . Thus these lines are assigned to the Ga(1) sites with  $\mathbf{B}^{\text{int}}=0$ .

To obtain the quadrupole parameters and the internal field that reproduce the frequencies of the remaining ten lines, we numerically diagonalized the hyperfine Hamiltonian; in this calculation we take  ${}^{69}\nu_Q$  as a fitting parameter and calculate  ${}^{71}\nu_Q$  from  ${}^{69}\nu_Q$  with the ratio  ${}^{69}Q/{}^{71}Q$ . We find that all the lines are assigned to only one type of Ga(2) sites as shown in Table III; this indicates that any nonequivalent Ga sites do not appear in the antiferromagnetic phase. The calculated resonance frequencies  $\nu_{\text{cal}}$  are shown in Fig. 3 (with calculated intensities) and Table III. The  $\nu_{\text{cal}}$  accurately agrees with  $\nu_{\text{obs}}$ ; the deviations are less than 0.01 MHz. For each of  ${}^{69}\text{Ga}$  and  ${}^{71}\text{Ga}$  nuclei, six resonance lines should be observed, but only five lines were in our measurement; this is reasonable because the calculated frequencies of the remain-

TABLE II. Quadrupole parameters for  ${}^{71}\text{Ga}$  nuclei and principal values of NMR shift tensor at 110 K.  ${}^{69}\nu_Q$  is deduced from  ${}^{71}\nu_Q$  with the ratio  ${}^{69}Q/{}^{71}Q = 1.5869$ .

|                      | Ga(1) | Ga(2) |
|----------------------|-------|-------|
| $K_X$ (%)            | 0.93  | 0.74  |
| $K_Y$ (%)            | 0.93  | 0.75  |
| $K_Z$ (%)            | 0.82  | 0.72  |
| ${}^{71}\nu_Q$ (MHz) | 11.38 | 16.30 |
| ${}^{69}\nu_Q$ (MHz) | 18.07 | 25.88 |
| $\eta$               | 0     | 0.145 |

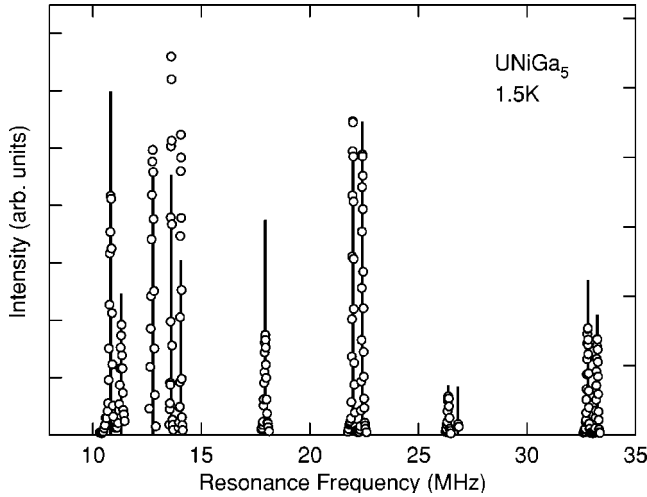


FIG. 3. Zero-field NMR spectrum at 1.5 K in the antiferromagnetic phase. Solid lines show the calculated frequency and intensity.

ing lines are about 0.44 MHz, out of range of our measurement.

The deduced quadrupole parameters and internal fields are listed in Table IV. The internal field at the Ga(2) sites lies along the  $Y$  axis, one of the principal axes of the field gradient. It is also found that for the Ga(2) sites,  $\nu_Q$  and  $\eta$  are almost unchanged from those in the paramagnetic phase.

#### IV. MAGNETIC STRUCTURE ANALYSIS

In this section, we search for the magnetic structure using the findings of our NMR measurements in the antiferromagnetic phase: (i) no additional nonequivalent Ga sites appear, (ii) for the Ga(1) sites  $\mathbf{B}^{\text{int}}=0$ , (iii) for the Ga(2) sites  $\mathbf{B}^{\text{int}}\parallel Y$ . The analysis is done in two steps. First, we determine the possible magnetic structures using the representation analysis from the propagation vector determined with the neutron diffraction. A considerable advantage of this method is that it systematically provides all the possible magnetic structures including multi- $\mathbf{k}$ , noncollinear, and incommensurate ones. Next, for each of the possible structures, we examine the magnetic site symmetry at the Ga sites and how the symmetry constrains the direction of the internal field. Then we determine the structures compatible with the findings of the NMR measurements.

In the tetragonal HoCoGa<sub>5</sub> structure, the propagation vector  $\mathbf{k}=\left[\frac{1}{2}\frac{1}{2}\frac{1}{2}\right]$  belongs to a single-arm star, and a unit cell contains only one U ion, then the magnetic-moment density is written as

$$\mathbf{m}(t_n) = \mathbf{m}_k \cos \mathbf{k} \cdot t_n, \quad (1)$$

where  $\mathbf{m}_k=(m_a, m_b, m_c)$  is a real polarization vector and  $t_n$  is the position vector of the  $n$ th unit cell. According to group representation theory, the moment density is expanded in terms of the basis functions of the small representations of the space group  $P4/mmm$  in the paramagnetic phase. Since this space group is symmorphic, the polarization vector is expanded in terms of the basis functions of the irreducible representations of the point group  $4/mmm(D_{4h})$ . Then the

TABLE III. Observed resonance lines in the zero-field spectrum and site assignment:  $\nu_{\text{obs}}$  is the observed frequency,  $\Delta$  is fullwidth at half-maxima, and  $\nu_{\text{cal}}$  is the calculated frequency.

| Site                | Line | $\nu_{\text{obs}}$ (MHz) | $\Delta$ (MHz) | $\nu_{\text{cal}}$ (MHz) |
|---------------------|------|--------------------------|----------------|--------------------------|
| <sup>71</sup> Ga(1) | 1    | 11.308                   | 0.13           | 11.303                   |
| <sup>69</sup> Ga(1) | 2    | 17.937                   | 0.10           | ...                      |
| <sup>69</sup> Ga(2) | ...  | ...                      | ...            | 0.436                    |
|                     | 3    | 10.821                   | 0.13           | 10.823                   |
|                     | 4    | 21.975                   | 0.08           | 21.974                   |
|                     | 5    | 22.417                   | 0.08           | 22.411                   |
|                     | 6    | 32.791                   | 0.09           | 32.797                   |
|                     | 7    | 33.233                   | 0.09           | 33.233                   |
| <sup>71</sup> Ga(2) | ...  | ...                      | ...            | 0.443                    |
|                     | 8    | 12.753                   | 0.14           | 12.754                   |
|                     | 9    | 13.614                   | 0.06           | 13.615                   |
|                     | 10   | 14.051                   | 0.06           | 14.059                   |
|                     | 11   | 26.373                   | 0.09           | 26.369                   |
|                     | 12   | 26.82                    | ~0.1           | 26.812                   |

representation induced by  $\mathbf{m}_k$  decomposes into irreducible representations as

$$\Gamma_{\mathbf{m}_k} = \Gamma_2^+ + \Gamma_5^+, \quad (2)$$

where  $\Gamma_2^+$  is a one-dimensional representation with the basis function (0,0,1) and  $\Gamma_5^+$  is a two-dimensional one with the basis functions (1,0,0) and (0,1,0). If we assume a second-order transition, the expansion of the moment density includes only a single irreducible representation; the assumption is justified by the smooth growth of the magnetic reflection intensity below  $T_N$ .<sup>10</sup> Then we find two types of possible structures: the  $\Gamma_2^+$  structure with  $\mathbf{m}_k\parallel c$  and the  $\Gamma_5^+$  structure with  $\mathbf{m}_k$  lying on the  $ab$  plane.

Next, consider constraints on the internal field direction at the Ga sites induced by the symmetry of these structures. Because internal fields are transformed as an axial vector by symmetry operations, inversion operations leave internal fields invariant and never induce such constraints on them. Since the magnetic structure described by the moment density, Eq. (1), is collinear, the magnetic symmetry can be described with magnetic space groups.<sup>14</sup> Based on them, we determine the magnetic site symmetry at the Ga sites and the constraints on the internal field below.

TABLE IV. Internal fields and quadrupole parameters at 1.5 K in the antiferromagnetic phase.

|                                | Ga(1)  | Ga(2)                   |
|--------------------------------|--------|-------------------------|
| <sup>71</sup> $\nu_Q$ (MHz)    | 11.303 | 16.443                  |
| <sup>69</sup> $\nu_Q$ (MHz)    | 17.937 | 26.094                  |
| $\eta$                         | 0      | 0.1467                  |
| $\mathbf{B}^{\text{int}}$ (kG) | 0      | 5.082 ( $\parallel Y$ ) |

TABLE V. Magnetic space group  $\bar{G}$ , magnetic point group, and the direction of  $\mathbf{B}^{\text{int}}$  at the Ga(1) site and the Ga(2) site at  $(\frac{1}{2}, 0, z)$ , for  $\Gamma_2^+$  and  $\Gamma_5^+$  structures.

|                      | $\mathbf{m}_k$                      | $\bar{G}$      | Ga(1)                        | Ga(2)                |
|----------------------|-------------------------------------|----------------|------------------------------|----------------------|
| $\Gamma_2^+$         | $(0, 0, m)$                         | $I4/m\bar{m}m$ | $4/m\bar{m}m$<br>$(0, 0, 0)$ | $2mm$<br>$(B, 0, 0)$ |
| Case I               | $(m, m, 0)$                         | $Ammm$         | $mmm$<br>$(B, B, 0)$         | 2<br>$(0, 0, B)$     |
| $\Gamma_5^+$ Case II | $(m, 0, 0)$                         | $Ammm$         | $mmm$<br>$(0, B, 0)$         | $2mm$<br>$(0, 0, B)$ |
| Case III             | $(m_a, m_b, 0)$<br>$(m_a \neq m_b)$ | $A2/m$         | $2/m$<br>$(B_a, B_b, 0)$     | 2<br>$(0, 0, B)$     |

The  $\Gamma_2^+$  structure has magnetic space group  $I4/m\bar{m}m$ , and magnetic point group is  $4/m\bar{m}m$  at the Ga(1) sites and  $2mm$  at the Ga(2) sites. For the Ga(1) sites, since  $C_2$  operation leaves the magnetic structure unchanged, it should also leave the internal field unchanged. But the operation actually transforms the internal field  $\mathbf{B}^{\text{int}} = (B_a, B_b, B_c)$  into  $(-B_a, -B_b, B_c)$ ; this indicates that  $B_a = B_b = 0$ . We also find  $B_c = 0$  from  $C_{2a}$  operation. As a result, the internal field must disappear at the Ga(1) sites in the  $\Gamma_2^+$  structure. For the Ga(2) site at  $(\frac{1}{2}, 0, z)$ ,  $\sigma_a$  operation leads to  $B_b = B_c = 0$  and the other magnetic symmetry operations do not induce any other constraints. Thus we conclude  $\mathbf{B}^{\text{int}} \parallel a$  at this Ga(2) site. In the same way, we find  $\mathbf{B}^{\text{int}} \parallel b$  at the Ga(2) site at  $(0, \frac{1}{2}, z)$ .

For the  $\Gamma_5^+$  structure, we consider three cases of the magnetic-moment direction separately,

- Case I  $\mathbf{m}_k = (m, m, 0)$ ,  
Case II  $\mathbf{m}_k = (m, 0, 0)$ ,  
Case III  $\mathbf{m}_k = (m_a, m_b, 0)$  ( $m_a \neq m_b$ ).

For Case I, the magnetic structure is orthorhombic  $Ammm$ . For Case II, the structure is also orthorhombic  $Ammm$ ; the Ga(2) sites are separated into two groups of nonequivalent sites with the same magnetic point group. For Case III, the structure is monoclinic  $A2/m$ , and the Ga(2) sites are also separated into two groups of nonequivalent sites with the same magnetic point group. For these three cases, we derive the constraints on the internal field in the same way as for the  $\Gamma_2^+$ . The results and the magnetic point group at the Ga sites are listed in Table V.

Our analysis shows that the  $\Gamma_5^+$  structure never fit the experimental finding that  $\mathbf{B}^{\text{int}} = 0$  at the Ga(1) sites. We therefore conclude that the magnetic structure is  $\Gamma_2^+$  with  $\mathbf{m}_k \parallel c$ . The  $\Gamma_2^+$  structure also agrees with the finding that no additional nonequivalent Ga sites appear in the antiferromagnetic phase. The orientations of the ordered moments and the internal field at the Ga(2) sites are shown in Fig. 4. This structure also agrees with the intensity analysis of the magnetic reflections.<sup>10</sup> For the Ga(2) sites, we have already found that  $\mathbf{B}^{\text{int}} \parallel Y$  from the analysis of the zero-field spectrum, hence the

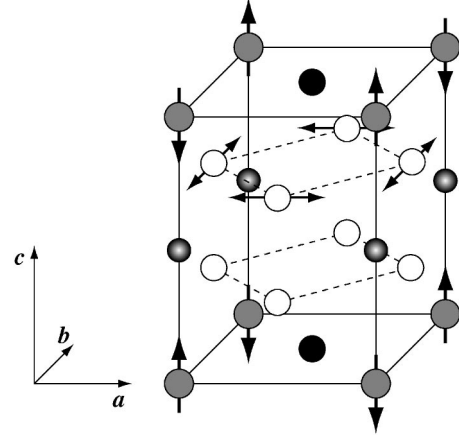


FIG. 4. The  $\Gamma_2^+$  magnetic structure of UNiGa<sub>5</sub>. Arrows show the directions of the ordered moment and the internal field at the Ga(2) sites.

$Y$  axis of the field gradient at the Ga(2)  $(\frac{1}{2}, 0, z)$  is along the  $a$  axis.

Although the present NMR analysis determined the magnetic structure of UNiGa<sub>5</sub>, it is not always possible for other magnetic structures. For example, unless nuclear sites have a symmetry operation that constrains the direction of internal fields, we cannot gain any information on the internal field from the present analysis. Nevertheless, this systematic analysis will be advantageous for reasons: one only needs the propagation vector to find possible magnetic structures, and as a result the analysis is independent of the intensity analysis of neutron magnetic reflections; and one need not know the details of hyperfine coupling.

Although we used magnetic groups to describe the magnetic symmetry for the collinear structure, one needs multi-color groups for noncollinear structures.

## V. SUMMARY

We measured the  $^{69,71}\text{Ga}$  NMR spectra in the paramagnetic and antiferromagnetic phases in the itinerant antiferromagnet UNiGa<sub>5</sub> and deduced the quadrupole parameters and the internal fields at the Ga(1) and Ga(2) sites. In the antiferromagnetic phase, we have found that no additional nonequivalent Ga sites appear and that the internal field at the Ga(1) sites disappears. We found possible structures with the representation analysis of magnetic structure from the propagation vector determined with the neutron diffraction. Each of the structures was examined if it fits to the findings of the NMR measurements, based on magnetic space groups, then we have determined a collinear magnetic structure with the magnetic moment along the  $c$  axis.

## ACKNOWLEDGMENTS

The authors thank H. Kadowaki for helpful discussion on the representation analysis of magnetic structure. This work was supported by Grand-in-Aid for Scientific Research from the Ministry of Education, Culture, Sports, Science and Technology.

\*Email address: ohama@nmr.s.chiba-u.ac.jp

- <sup>1</sup>A. Abragam, *The Principles of Nuclear Magnetism* (Oxford University Press, Oxford, 1961).
- <sup>2</sup>T. Ohama, A. Goto, T. Shimizu, E. Ninomiya, H. Sawa, M. Isobe, and Y. Ueda, *J. Phys. Soc. Jpn.* **69**, 2751 (2000).
- <sup>3</sup>E. F. Bertaut, *Acta Crystallogr., Sect. A: Cryst. Phys., Diffraction, Theor. Gen. Crystallogr.* **24**, 217 (1968).
- <sup>4</sup>Y. A. Izyumov, V. E. Naish, and R. P. Ozerov, *Neutron Diffraction of Magnetic Materials* (Plenum, New York, 1991).
- <sup>5</sup>H. Kadowaki, *J. Phys. Soc. Jpn.* **67**, 3261 (1998).
- <sup>6</sup>Y. N. Grin, P. Rogl, and K. Hiebl, *J. Less-Common Met.* **121**, 497 (1986).
- <sup>7</sup>K. Kaneko, N. Metoki, N. Bernhoeft, G. H. Lander, Y. Ishii, S. Ikeda, Y. Tokiwa, Y. Haga, and Y. Onuki, *Phys. Rev. B* **68**, 214419 (2003).
- <sup>8</sup>S. Noguchi and K. Okuda, *J. Magn. Magn. Mater.* **104–107**, 57 (1992).
- <sup>9</sup>K. Okuda and S. Noguchi, *JJAP Ser.* **8**, 32 (1993).
- <sup>10</sup>Y. Tokiwa, Y. Haga, N. Metoki, Y. Ishii, and Y. Onuki, *J. Phys. Soc. Jpn.* **71**, 725 (2002).
- <sup>11</sup>M. H. Cohen and F. Reif, *Solid State Phys.* **5**, 321 (1957).
- <sup>12</sup>M. I. Valič and L. I. Williams, *J. Phys. Chem. Solids* **30**, 2337 (1969).
- <sup>13</sup>H. Kato (private communication).
- <sup>14</sup>M. Tinkham, *Group Theory and Quantum Mechanics* (McGraw-Hill, New York, 1964).